

# Soft Matter

Accepted Manuscript



This is an *Accepted Manuscript*, which has been through the Royal Society of Chemistry peer review process and has been accepted for publication.

*Accepted Manuscripts* are published online shortly after acceptance, before technical editing, formatting and proof reading. Using this free service, authors can make their results available to the community, in citable form, before we publish the edited article. We will replace this *Accepted Manuscript* with the edited and formatted *Advance Article* as soon as it is available.

You can find more information about *Accepted Manuscripts* in the [Information for Authors](#).

Please note that technical editing may introduce minor changes to the text and/or graphics, which may alter content. The journal's standard [Terms & Conditions](#) and the [Ethical guidelines](#) still apply. In no event shall the Royal Society of Chemistry be held responsible for any errors or omissions in this *Accepted Manuscript* or any consequences arising from the use of any information it contains.



Journal Name

ARTICLE

## Supramolecular Polyelectrolyte Complex (SPEC): pH Dependent Phase Transition and Exploitation of its Carrier Properties

Received 00th January 20xx,  
Accepted 00th January 20xx

DOI: 10.1039/x0xx00000x

www.rsc.org/

Subharanjan Biswas,<sup>a</sup> Ethayaraja Mani,<sup>b</sup> Arobendo Mondal,<sup>c</sup> Ashwani Tiwari<sup>c</sup> and Soumyajit Roy<sup>\*a</sup>

A Supramolecular Poly-Electrolyte Complex (SPEC) comprising of poly-electrolyte Acrylic acid with supramolecularly complexed Guanidium is reported. This complex shows pH responsive phase transitions, which are described and characterized using microscopy, spectroscopy, density functional theory studies & Monte Carlo simulations. The phase behaviour of the SPEC is exploited by loading a dye like perylene and a drug viz., doxorubicin and their pH dependent controlled release is demonstrated, courtesy: the pH dependent phase change of the SPEC.

### Introduction

Phase transitions in various model systems<sup>1-5</sup> are of interest to materials science to understand various phenomena<sup>6</sup> and emergence of new properties in materials.<sup>7-10</sup> Hence choice of a model system is important to exploit such emergence of novel properties in materials. Systems such as soluble polymer – colloid dispersion mixtures show a rich phase behaviour<sup>11-17</sup> and may serve as an interesting model system as they provide a window to evidence emergence of new materials on molecular as well as mesoscopic length-scales.<sup>18-24</sup> Such polymeric materials have been moulded into materials with nanoscopic morphologies and have been used in nanolithography, organic photovoltaics, batteries etc.<sup>25</sup> Thus understanding the phase behaviour of soluble polymers and polymer-colloid has been received immense importance. Such phase behaviour has also been explained in the light of hard sphere interaction with certain stickiness and parallel has been drawn with the phase behaviour of another ubiquitous liquid water.<sup>12</sup> Likewise, Inter-Polyelectrolyte Complexes (IPECs) comprising of charged polymeric complexes have been shown to demonstrate interesting behaviour on changing external conditions and associative phenomena due to conformational change on molecular level.<sup>26-31</sup> Very recently using broad band dielectric spectroscopy (BDS) and nanoelectrode glassy

dynamics of tiny volume of an isolated polymer chain has been shown to be identical to that observed in the bulk.<sup>32</sup> Question arises, is it possible to observe related interesting colloid polymer phase phenomena using a single polyelectrolyte and a supramolecular additive? Do they form supramolecularly organised states or Supramolecular Polyelectrolyte Complexes (SPECs)<sup>33-35</sup> that can be switched from polymeric to colloidal state by means of an external trigger like pH?

Here, we have studied such a model system comprising of Polyacrylic acid with a supramolecular cross linker Guanidium. This system comprises of polymeric strings of Polyacrylic acid (abbreviated as PAA here onwards) with patchy<sup>36-38</sup> hydrogen bonding sites on it. In general the sites are inactive or non-sticky and do not show any interesting phase behaviour,<sup>39-41</sup> but as soon as we add Guanidium (abbreviated as GD in the study) to it and pH<sup>42-44</sup> is increased, a white turbidity appears in the colourless mixture. On further increment in pH, turbidity goes on increasing and after certain pH it forms a gel-block and gets separated from clear solution. We have found this phenomenon to be totally reversible, as on decreasing pH, the gel block starts to get dissolved in the solution and totally dissolves when pH is completely reversed. We have further exploited this reversibility in controlled release of substrates like a dye or a drug.

Now, the errand is to find out the phenomenon behind such reversible phase transition and to correlate this phenomenon with molecular level interaction among PAA and GD. PAA as well as GD comprise of numerous hydrogen bonding sites. So, is there any role of supramolecular interaction<sup>45-47</sup> behind the phase behaviour of our system? Can we envisage formation of supramolecularly structured phases being assembled and disassembled in this system with an external trigger<sup>48-54</sup> like

<sup>a</sup> Eco-Friendly Applied Materials Laboratory, Department of Chemical Sciences, New Campus, IISER-Kolkata, India. Fax: +91 3325873020; Tel: +919007222901; E-mail: s.roy@iiserkol.ac.in, roy.soumyajit@googlemail.com.

<sup>b</sup> Polymer Engineering & Colloid Science Group, Department of Chemical Engineering, Indian Institute of Technology - Madras, Chennai - 600036, India.

<sup>c</sup> Department of Chemical Sciences, IISER-Kolkata, India.

Electronic Supplementary Information (ESI) available: [Molecular weight distribution curve of PAA is included in ESI]. See DOI: 10.1039/x0xx00000x

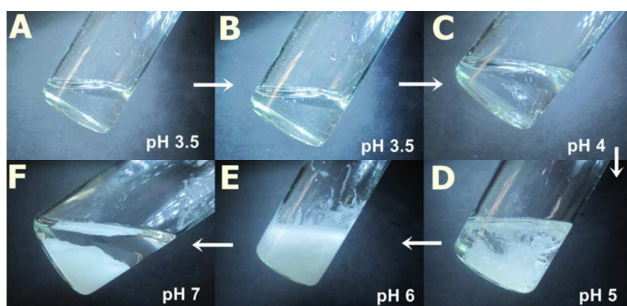


Figure 1. Images of phase change and complete phase separation. Only liquid phase exists in PAA and PAA-GD (Figure 1A & 1B respectively) continuous phase transfer takes place on increasing pH resulting PAA-GD cluster (1C to 1E). Complete separation of liquid and gel phase (PAA-GD gel) is shown in 1F.

the variation of pH?<sup>55, 56</sup> If so, can such phenomenon be exploited for controlled release of substrates like dyes and drugs? We answer these questions here.

## Experimental Section

Acrylic acid, Sodium hydroxide used in this study are of reagent grade. All other chemicals are analytical grade. Guanidinium hydrochloride is purchased from Sigma Aldrich, Germany. All other reagents are purchased from Merck, Germany. The reagents are used as obtained without further purification.

### Synthesis of low molecular weight PAA

60 g deionized water and 2 g Sodium hydrogen sulfite are added into a reactor and stirred until dissolved. The reactor then is slowly heated in an oil-bath and temperature is raised to 60 °C. Afterwards, a mixture of 20 g acrylic acid, 0.2 g Ammonium peroxydisulphate and 20 mL deionized water is mixed and fed into the reactor by adding the whole mixture drop by drop over 40 minutes. The solution is stirred at 60 °C for another 1.5 hours. Later on, the reactor is cooled and the PAA so obtained is used for further experiments as described in the text.

### Preparation of PAA-GD composite, cluster and the gel block

The as prepared PAA is used as a starting material for the synthesis of supramolecularly cross-linked patchy polymeric material. 4 g low molecular weight PAA is taken in a sample vial; different weight percentages of Guanidinium hydrochloride (5% (0.2 g), 10% (0.4 g), 15% (0.6 g), 25% (1.0 g), 35% (1.4 g), 45% (1.8 g), 55% (2.2 g)) are added into PAA. The samples are then ultrasonicated until GD completely dissolves into PAA. 7.5 mol/L NaOH is added into the solution drop by drop to increase the pH of the sample to get to the first cloud point. After continuous increment of pH, white gel block is formed by complete phase separation. We then reverse the pH to dissolve the gel block to obtain the liquid phase again. We have used 10% PAA-GD here onwards as reference for other experiments.

### Gel Permeation Chromatography (GPC)

Consenxus GmbH GPC system was used to measure the molecular weight and molecular weight distribution of the

synthesized PAA. 1 mg/ml PAA concentration was injected in the system fitted with a RI detector.

### Study of Density Functional Theory and Monte Carlo Simulation

The molecular geometries are optimized at B3LYP/6-31g level using Gaussian 09 package.<sup>57</sup> Details of the result have been explained in result and discussion section. Monte Carlo simulation study is also discussed in detail in result and discussion section.

### Spectroscopy and microscopy experiments

UV-Visible spectra are recorded in the range 200–1000 nm with a Shimadzu UV-160A spectrophotometer and evaluated with a program associated with the spectrometer. A LABRAM HR800 Raman spectrometer is employed using the 633 nm line of a He-Ne ion laser as the excitation source to analyse the sample. FTIR spectra reported in this study are recorded with a Perkin Elmer Spectrum RX1 spectrophotometer with HATR (Horizontal Attenuated Total Reflectance) facility in the range 4000–500 cm<sup>-1</sup>. SEM (Scanning Electron Microscopy) and Cryo-SEM images are acquired by a Zeiss Sigma microscope. All the gel samples were first dried in vacuum for 2 days prior to SEM experiments. Cryo-SEM was done using samples as it were. TEM (Transmission Electron Microscopy) images are taken with a JEOL JEM 2010 electron microscope. Gel samples were first properly diluted with milli-Q water, then drop-casted on 300 mesh TEM grid prior to TEM experiments.

### Rheological studies

To understand the viscoelastic properties of gels, we have performed rheological experiments on a rheometer (AR-G2, TA Instruments). All the experiments were carried out at 25 °C using 40 mm steel parallel plate with plate gap of 1.0 mm. Storage modulus ( $G'$ ) and loss modulus ( $G''$ ) of the gels have been recorded in the linear viscoelastic regime at a shear strain of  $\gamma = 2\%$  with angular frequency sweep.

### Loading and controlled release of Perylene-3,4,9,10-tetracarboxylate and Doxorubicin hydrochloride by PAA-GD gel phase

5 mg Perylene-3,4,9,10-tetracarboxylate<sup>58</sup> (abbreviated as PTC here onwards) has been added to 4 ml PAA-GD 10% solution. The mixture has been ultrasonicated using a Takashi Ultrasonicator until dissolved. PTC loaded PAA-GD is then subjected to pH variation from 4 to 7 till complete phase separation takes place. After that, the gel phase has been dissolved by reversal of pH.

In case of Doxorubicin hydrochloride (Dox), 2 mg Dox has been mixed with 4 ml PAA-GD 10% solution and ultrasonicated till it dissolves completely. pH of the mixture is then varied to get the separated phase and then reversed to initial pH dissolving the gel phase. Both PAA-GD-PTC as well as PAA-GD-Dox at different pH has been investigated by Confocal Microscopy and Scanning electron Microscopy.

## Results and Discussions

Molecular weight and molecular weight distribution of the synthesized PAA was measured by gel permeation

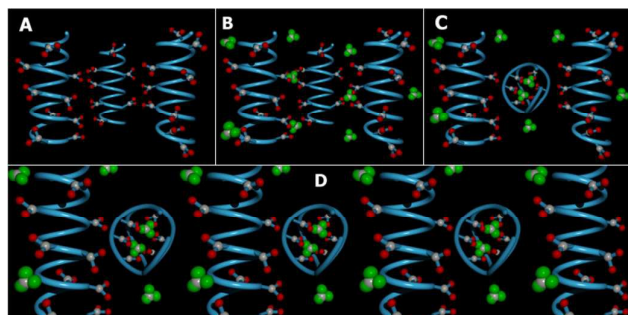


Figure 2. 3D depiction of model PAA-GD networks. In Figure 2A blue PAA chains are shown, COOH groups are shown in ball and stick model (in red and grey) attached to blue PAA chains. Figure 2B depicts PAA-GD supramolecular interactions, where GD, shown in green space-filling triangles act as cross-linkers (PAA-GD liquid). At elevated pH PAA-GD clusters form with GD trapped inside PAA coil, as shown in Figure 2C. Figure 2D shows phase separated PAA-GD clusters inside PAA network forming the gel.

chromatographic (GPC) experiment (See SI). Molecular weight of PAA was calculated to be 7000 Da from GPC measurements. We have shown earlier that using supramolecular interactions it is possible to induce gelation in PAA network.<sup>59</sup> Now we proceed on to the next step using one such supramolecular linkage unit like GD. We explore in this study the effect of change of pH in the supramolecular cross-linking network of PAA-GD and the phase behaviour<sup>60</sup> of that particular system on changing pH. For instance, at the beginning of the experiment, there is a clear liquid phase of PAA having pH nearly equal to 3.5 (Figure 1A). We add GD to it with no significant change in pH, only the media becomes more viscous (Figure 1B). Afterwards, we add NaOH solution (7.5 mol/L) drop-wise. At pH 4, we see the appearance of white cloud and at this point coexistence of liquid as well as cloudy phase is visible (Figure 1C). As pH is further elevated, formation of more turbidity is found to occur (Figure 1D). At pH nearly equal to 6, maximum turbidity is found (Figure 1E). Separation of phases takes place thereafter on increasing pH further. At this stage (pH ~ 7), a gel completely separates out forming clear liquid in the supernatant (Figure 1F).

We now construct a simple model to explain the above experimental observations. Our model is that of a patchy polymer. It further has patchy triangular blocks representing GD which can be modulated with changing pH (Figure 2). We now explain the observations based on this model.

Initially, there are small polymeric chains of PAA, well soluble in water to form a viscous solution (Figure 1A & 2A). Now, to this solution we add GD having 6 dormant hydrogen bonding sites, which can be activated upon increasing pH by the addition of NaOH. Upon increasing pH, deprotonation of PAA network takes place prior to GD, due to its lower pKa value (4.25) with respect to GD (pKa 13.6) which results in supramolecular connection formation between PAA and GD (PAA-GD liquid, Figure 1B & 2B). Later on, with further increase in pH, coiling of polymeric chains take place due to a favorable conformational change in the polymeric network.<sup>61</sup> At this stage, a few PAA chains start wrapping up supramolecularly linked GD inside and forms polymer coils leading to the formation of the white turbidity which is the PAA-GD cluster

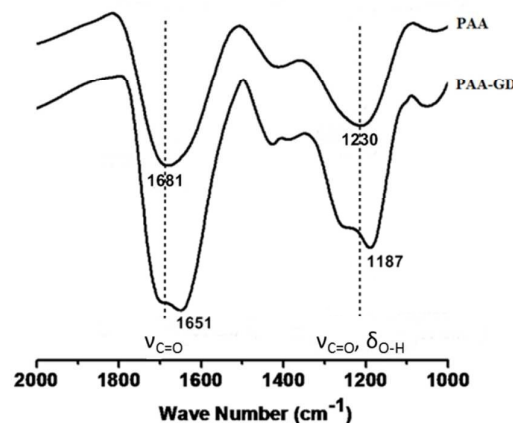


Figure 3. Infrared spectroscopic signatures of PAA and PAA-GD cluster. Blue shift is seen from PAA to PAA-GD for C=O stretching frequency ( $1681\text{ cm}^{-1}$  in PAA) as well as for C-O stretching coupled with O-H bending ( $1230\text{ cm}^{-1}$  in PAA) which indicates hydrogen bonding in PAA-GD network.

phase (Figure 1C & 2C). Clustering gradually increases with increase in pH and finally forming a white gel, which gets separated out from solution (PAA-GD gel phase, Figure 1F & 2D). At low pH soluble polymeric networks have dominance over clustering which is due to the fact that only few deprotonated PAA and protonated GD are present under this condition. Upon reaching a pH value of around 6, the cluster formation increases significantly. On further increasing the pH to 7, there is a clear phase separation (Figure 1F & 2D).

This transition is sharply visible as there is a clear phase separation at pH 7. At this point the PAA-GD cluster formation reaches maximum and those insoluble clusters get separated out as white gel (Figure 1F & 2D). Formation of PAA-GD cluster from PAA is verified by FTIR spectroscopic experiments.

We now investigate the gels by ATR-FTIR spectroscopic experiments (Figure 3). Distinct differences in spectral signatures are observed between the starting PAA and PAA-GD cluster networks, implying effective supramolecular cross-linking in the latter. The PAA-GD cluster networks show a blue shift in the spectral signature of the carboxylate groups from  $1681\text{ cm}^{-1}$  to  $1651\text{ cm}^{-1}$  implying a stiffening of the corresponding bonds due to hydrogen bonding in the PAA-GD cluster networks (Figure 3). More precisely, in the case of PAA-GD clusters, an intense peak is observed at  $1651\text{ cm}^{-1}$  while in free PAA this peak is observed at  $1681\text{ cm}^{-1}$ . This is due to intermolecular hydrogen bonding of the C=O groups in the PAA with NH- of GD in the cross-linked polymer causing the blue shift in the stretching frequency of the C=O bond of PAA in PAA-GD network. Stretching frequencies at  $1230\text{ cm}^{-1}$  corresponding to C-O stretching coupled with O-H bending in the case of pristine PAA is blue shifted to  $1187\text{ cm}^{-1}$  in the PAA cross-linked with GD. The above shifts thereby show the presence of a more rigid hydrogen bonded or supramolecularly connected network in the PAA-GD cross-linked polymeric network. These infrared spectroscopic results indeed prove the formation of a supramolecular network with

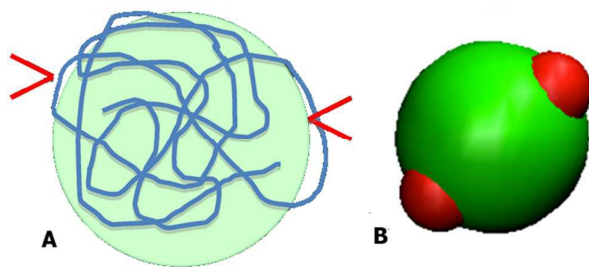


Figure 4. Schematics of PAA polymer in coil form with two bound GD (4A) and an equivalent patchy model (4B).

PAA-GD where GD acts as a supramolecular cross-linker to PAA polymeric chains.

Here, it is worth mentioning that supramolecular interaction plays a crucial role in formation of networks inside the polymer as well. A huge number of free hydrogen bonding sites in both PAA and GD increase the possibility of network formation. When complete phase separation takes place the gel block material is obtained.

We conclude this step to be comprising of polymeric network matrix with coiled up PAA chains encapsulating GD units, glued together by GD units. Now we describe the behaviour of the entire system by a patchy polymer model using Monte Carlo simulations.

Both PAA and GD have been partially deprotonated under the studied experimental conditions. Under these conditions, it is likely that PAA acquires a coiled conformation and PAA-GD network is formed due to hydrogen bonding. This is shown in Figure 4A, where the red arrows indicate the attachment of GD with PAA polymer at random sites.

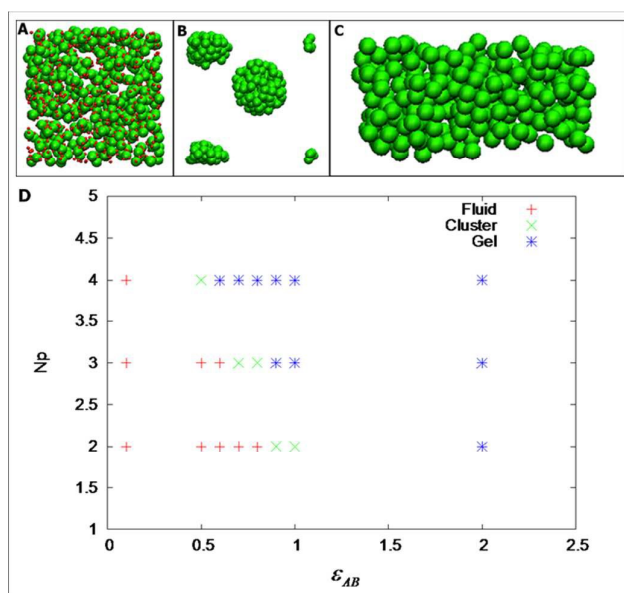


Figure 5. Representative snap shots in Monte Carlo Simulation of fluid (5A), cluster (5B) and gel (5C) phases. Patches are shown only in 5A. 5D is the Phase diagram at a polymer volume fraction of 0.105.

We have considered such a network of a soft polymer sphere and sticky patches as shown in Figure 4B. The green balls (here abbreviated as A) are the squishy polymer region of PAA and the red patches (abbreviated as B) are the locations of GD. We have also assumed that between two patchy polymer spheres, green-red (A-B) parts interact via hydrogen bond, red-red (B-B) parts repel due to electrostatic interactions, and green-green (A-A) parts interact with a soft potential model. The overall sum of the inter-polymer potentials is mathematically given as:

$$U_{AA}(r) = \epsilon_{AA} \left( \frac{\sigma_A}{r} \right)^6 \quad 0 < r < \infty \quad (1)$$

$$U_{BB}(r) = \epsilon_{BB} \left( \frac{\sigma_B}{r} \right)^6 \quad r < \sigma_B$$

$$= \frac{\epsilon_{BB} \sigma_B}{r} e^{-\left( \frac{r - \sigma_B}{\xi_{BB}} \right)} \quad \sigma_B \leq r \quad (2)$$

$$U_{AB}(r) = \epsilon_{AA} \left( \frac{\sigma_A + \sigma_B}{2r} \right)^6 \quad r < (\sigma_A + \sigma_B)/2$$

$$= \frac{\epsilon_{AB} \sigma_{AB}}{r} e^{-\left( \frac{r - (\sigma_A + \sigma_B)/2}{\xi_{AB}} \right)} \quad (\sigma_A + \sigma_B)/2 \leq r \quad (3)$$

In the above equations (Equation 1, 2 & 3)  $\epsilon_{AA}$ ,  $\epsilon_{AB}$  and  $\epsilon_{BB}$  are the parameters denoting strength of pair interactions,  $\sigma_A$  and  $\sigma_B$  are the diameters of the polymer part and patch diameter,  $\sigma_{AB}$  is the arithmetic mean of  $\sigma_A$  and  $\sigma_B$ .  $\xi_{BB}$  and  $\xi_{AB}$  are the screening lengths. We have scaled all the length scales with  $\sigma_A$  and energy scales with  $k_B T$ , where  $k_B$  is Boltzmann constant and  $T$  is temperature.

Some parameters have been fixed to a certain value like  $\epsilon_{AA} = 2$ ,  $\epsilon_{AB} = 2$ ,  $\xi_{AB} = 1$ ,  $\xi_{BB} = 0.1$ ,  $\sigma_B = 0.1$ . We have studied the effect of number of patches ( $N_p$ ) and  $\epsilon_{AB}$ , which are related to the amount of GD and strength of hydrogen bonding, respectively. These two parameters can be directly adjusted in the experiments. We have performed NVT Monte Carlo simulations with 500 patchy particles using cubic periodic boundary conditions with Metropolis algorithm. While starting up the simulation,  $N_p$ , number of patches has been randomly distributed on the surface of the polymer particle. In the simulation, a particle is randomly chosen and given a translational displacement and rotational displacement using quaternion. The step has been accepted according to the Metropolis acceptance rule:  $e^{-(E_n - E_o)/K_B T}$ , where  $E_n$  and  $E_o$  are the total potential energies after and before the random move. This is continued until the equilibrium is attained.

For a fixed density, we have varied  $N_p$  and  $\epsilon_{AB}$ . Figure 5A, 5B, 5C shows the phase diagram of the patchy model for volume fraction of 0.105. As shown in Figure 5D, we have observed that at low values of  $N_p$  and  $\epsilon_{AB}$ , the particles are fluid-like.

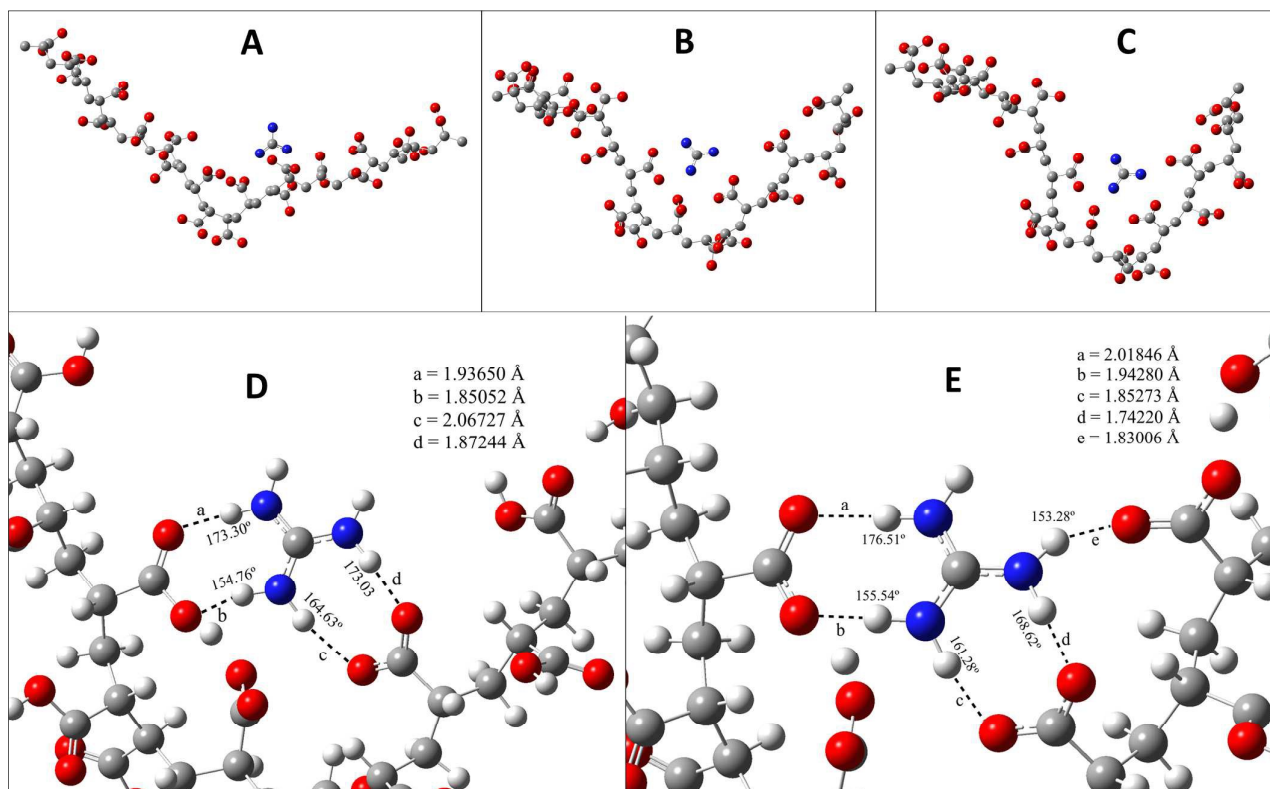


Figure 6. Details of DFT studies have been depicted. In Figure 6A, oxygen atoms of the COOH group form hydrogen bonds with N-H of GD molecules. Figure 6B and 6C show the gradual increase in interaction among GD and PAA inside a single PAA chain with increase in number of free  $\text{-COO}^-$  and this enhanced interaction results in coiling of the PAA forming PAA-GD cluster. D and E are the close up views of B and C respectively where the hydrogen bonded distances are shown. It is clearly seen that most of the hydrogen bonds are getting shortened and formation of more hydrogen bonds are also seen with enhanced interaction between PAA and GD.

Upon increasing either  $N_p$  or  $\epsilon_{AB}$ , we have observed a stable cluster phase (the PAA-GD coiled state). There is a well-defined fluid-cluster boundary, which can be traced either by increasing  $N_p$  with fixed  $\epsilon_{AB}$  or vice-versa. This implies reversibility in formation of various phases as observed experimentally. Representative snapshots of the fluid (PAA-GD liquid), cluster (PAA-GD phase) and gel phase (phase separated PAA-GD gel) are shown in Figure 5.

With a simple coarse-grained model, we have shown the fluid-cluster-gel transitions in the simulation, which qualitatively confirms the experimental data (Figure 5). The simulation results do confirm our hypotheses that there are hydrogen bonding interactions between PAA polymer and GD additive. We make no attempt to quantitatively compare the results between experiments and simulation, as the level of coarse-graining of PAA polymer is far too unspecific. However, the qualitative agreement between experiments and our calculations is obvious.

Now we take a closer look at the phase behaviour of our system in the molecular level. To do so we have taken resort to Density Functional Theory (DFT) and here we describe the results obtained by DFT. The monomer of PAA has  $\text{-COOH}$  group which is sensitive to the pH of the solution. When the solution is acidic the  $\text{-COOH}$  group remains in neutral form, as the pH increases the number of  $\text{-COO}^-$  ions in solution

increases. Protonated GD unit is able to form hydrogen bond with  $\text{-COO}^-$  group of PAA. In Figure 6A, it is shown that the oxygen atom of the  $\text{-COO}^-$  group forms hydrogen bond with N-H of GD units. It is quite clear that there are many N-H-O hydrogen bonds. As the pH value of solution increases the  $\text{-COO}^-$  ions starts forming. Figure 6B (& D) and 6C (& E) shows that as the number of  $\text{-COO}^-$  ions increases in the polymer the attraction between the protonated GD and PAA increases. This forces the polymer to get coiled as PAA-GD cluster. Also upon increasing pH, interaction between the PAA with GD increases, this reduces the intermolecular interaction of the polymer with others, with the result that polymer makes a separate phase of aggregated cluster i.e. the PAA-GD gel phase.

From the previous discussion it is clear that PAA network has free chains and those that are connected via GD units form coils on deprotonation of the PAA network. At the beginning of the experiment, there are free PAA chains (Figure 1A & 2A). Addition of GD results in supramolecular connection formation between the PAA chains leading to the formation of network of supramolecular polymeric chains by mediation of GD (Figure 1B & 2B). On addition of base, a few of the supramolecular bonding sites of PAA (carboxylic acid groups) as well as GD (imine and amine groups) get deactivated due to deprotonation. Such deprotonation of PAA and GD results in destruction of some supramolecular cross linking within PAA-

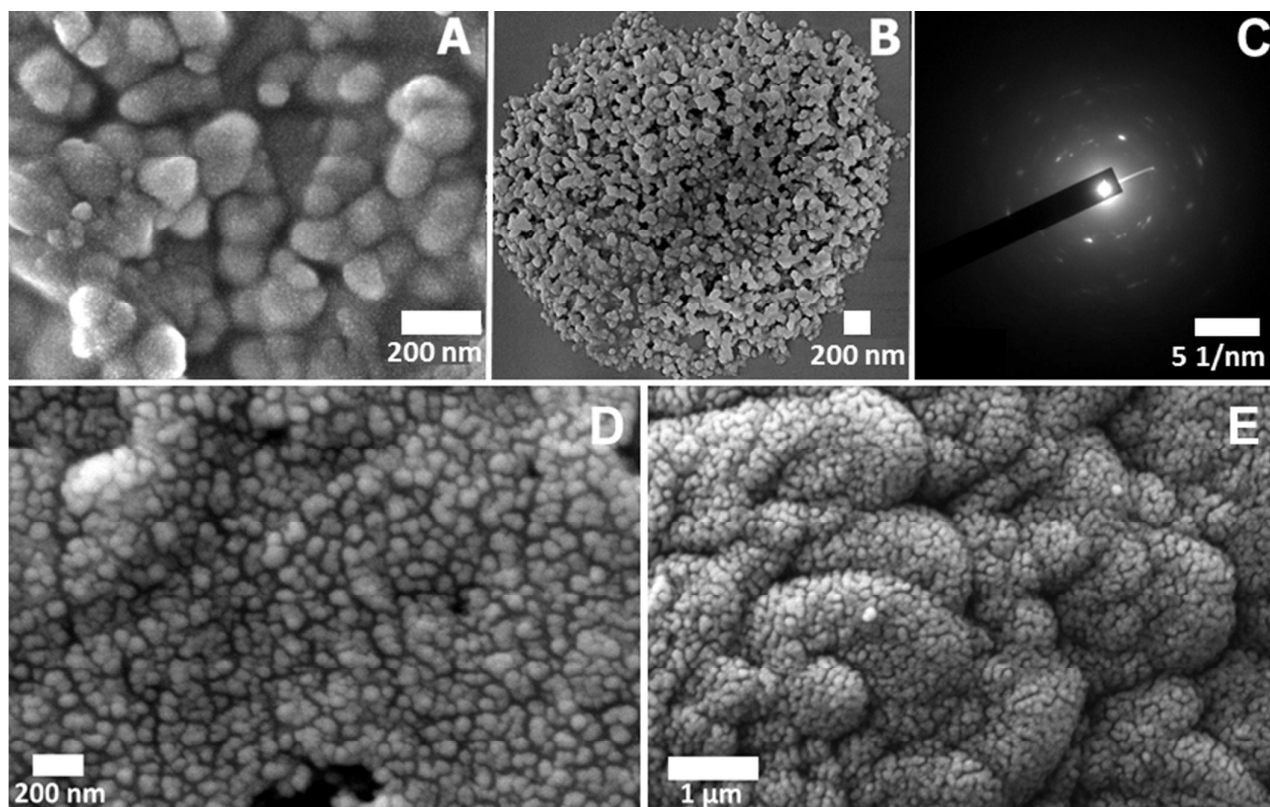


Figure 7. 7A and 7D are the SEM and Cryo-SEM images respectively for the appearance of first cloud point. Spherical coiled structure of polymeric network at the formation of gel block is clearly visible from SEM and Cryo-SEM (7B and 7E respectively). 7C shows Transmission Electron Microscopy Selected Area Electron Diffraction (SAED) pattern of the separated PAA-GD gel block at pH 7 showing discrete spots indicating ordered lattice like structure in that gel-block.

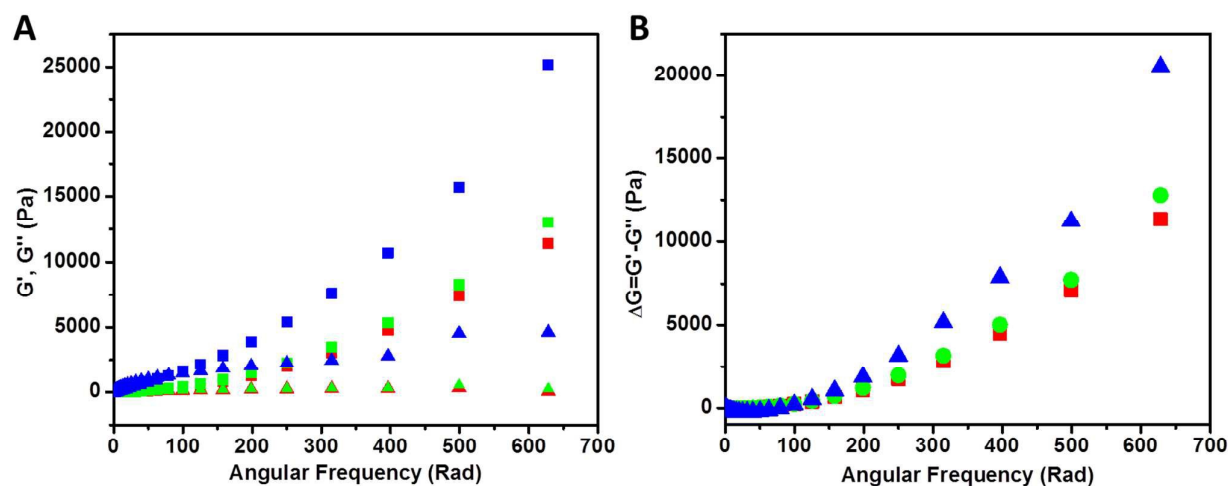


Figure 8. (A) Storage modulus ( $G'$ , square) and loss modulus ( $G''$ , triangle) data of PAA (red), PAA-GD composite (green) and PAA-GD gel block (blue) at 2% constant strain. (B) Difference of storage and loss modulus with angular frequency, PAA (red), PAA-GD composite (green) and PAA-GD gel block (blue).  $G' > G''$  found in all cases indicate the rheological behavior in the gel samples dominated by an elastic property rather than a viscous property.

GD liquid network. PAA as well as GD still have some hydrogen bonding sites intact. Those active hydrogen bonding sites of PAA as well as GD help PAA chains to wrap forming a coil with supramolecularly linked GD inside it. In short, PAA-GD cluster

formation takes place when a polymeric chain of PAA gets coiled up on an external trigger (here, pH) with cross-linkers (GD) inside it (Figure 1C & 2C).

Phase transition phenomenon is also clearly visible from microscopic studies. Network formation at appearance of

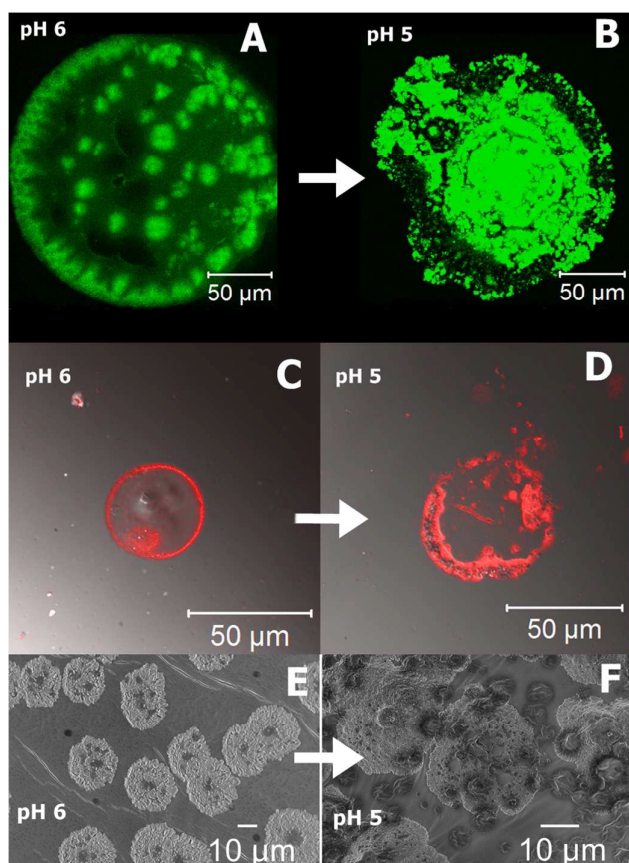


Figure 9. Confocal Microscopic images of pH dependent controlled release of PTC (A and B) and Dox (C and D). SEM snap shots of PTC release from the cluster at different pH (E and F).

cloud point is seen (Figure 7A). Scanning electron microscopic image at pH 4 of first cloud point clearly shows the network structure of PAA-GD clusters. Figure 7B shows phase separation at final cloud point at pH 7 where the PAA-GD clusters are all assembled together and gets separated as PAA-GD gel. This is also evident from cryo-SEM images. Figure 7D represents the appearance of cloud point and image 7E is the separated cluster phase.

In Transmission Electron Microscopic Selected Area Electron Diffraction (SAED) pattern, at pH 7, we see regular diffraction pattern with discrete spots indicating ordered lattice like structure formation within the phase separated white gel – the PAA-GD gel, just as we observe in a crystalline material. Hence it proves our proposition that lattice like structure forms as soon as we change the pH of the polymeric system and separated PAA-GD gel has a regular lattice in its interior structure.

Rheological study of the samples has been shown in figure 8. Storage modulus  $G'$  (closed symbols) and loss modulus  $G''$  (open symbols) values of PAA (red), PAA-GD composite (green) and PAA-GD cluster gel block (blue) has been shown with function of angular frequency. We observed higher value of storage modulus ( $G'$ ) than the loss modulus ( $G''$ ) within the linearity limits of deformation, indicating the rheological

behavior in the gel is dominated by an elastic property rather than a viscous property.

The pH induced phase transition of PAA-GD cluster to PAA-GD gel and liquid PAA-GD is reversible. We now exploit this reversible transition<sup>62-64</sup> of PAA-GD cluster to PAA-GD gel and PAA-GD liquid phases for loading of substrates and their controlled release. As we reverse the pH at each step of cluster formation, the turbidity disappears to break the PAA-GD cluster. Below pH 4, only liquid phase exists (PAA-GD liquid), whereas between pH 4-6, existence of cluster phase (PAA-GD cluster) is evidenced. On the other hand, at pH > 6, there is only Gel phase: PAA-GD gel.

The cross-linked polymer PAA-GD liquid is first loaded with Perylene-3,4,9,10-tetracarboxylate (PTC) and then with Doxorubicin hydrochloride (Dox). Both PAA-GD-PTC as well as PAA-GD-Dox are subjected to pH variation. At pH 7 phase separation takes place for both cases. Reversal of pH homogenizes the separated phases. All the variations are examined by Confocal Microscopy and Scanning Electron Microscopy. When the pH of the gel block (formed at pH 7) loaded with PTC is reduced to pH 6, we see green fluorescence of PTC confined within the gel network as shown in Figure 9A. With further reduction of pH, (at pH 5) this gel network disassembles with the concomitant release of PTC (Figure 9B). PAA-GD-Dox has shown the same characteristics with red fluorescence (Figure 9C & 9D). In other words on reducing pH, Dox is released from PAA-GD-Dox network. SEM images also justify and show similar results where we can see a clear picture of dye loading (Figure 9E) and release (Figure 9F).

## Conclusions

To summarize, we have demonstrated pH triggered phase transition of a supramolecular polyelectrolyte complex by formation of supramolecular connectivity within polymeric network by spectroscopic and microscopic techniques taking PAA and GD mixture as a model system. We observe that initially clear PAA solution becomes viscous when mixed with GD. Upon increasing the pH slowly to pH 4, initial turbidity appears. The turbidity keeps on increasing with pH. We explain this behaviour with the aid of DFT and MC simulations and explain it as a result of formation of coiled SPECS from PAA-GD networks. We also observe that this pH induced phase transition is reversible in nature. In other words it is possible to move from a liquid (PAA-GD) phase state to cluster (coiled PAA-GD) state, and reverse. Thus, we exploit this reversibility to load fluorescent molecule like Perylene-3,4,9,10-tetracarboxylate and drug molecule like Doxorubicin hydrochloride and show their pH dependent uptake and release. Scopes are open to modify and use such systems as controlled drug delivery agents inside infected human cells.

## Acknowledgements

Cooperation of Dr. Subi Jacob George, K. Venkata Rao, Dandan Yuan and Rongxin Yuan is gratefully acknowledged. Dr. Raja



Shunmugam is thanked for providing us with Doxorubicin hydrochloride. We acknowledge the help of Ritabrata Ghosh of IISER-Kolkata for Confocal Microscopy. SR thanks DST fast track, BRNS-DAE grant, IISER-Kolkata & CIT for start-up grants. SB thanks UGC-SRF for scholarship.

## Notes and references

<sup>a</sup> Eco-Friendly Applied Materials Laboratory, Department of Chemical Sciences, IISER-Kolkata, India. Fax: +91 3325873020; Tel: +919007222901; E-mail: s.roy@iiserkol.ac.in, roy.soumyajit@googlegmail.com.

<sup>b</sup> School of Chemistry and Materials Engineering, Changshu Institute of Technology, Changshu, P. R. China.

<sup>c</sup> Polymer Engineering & Colloid Science Group, Department of Chemical Engineering, Indian Institute of Technology - Madras, Chennai - 600036, India.

<sup>d</sup> Department of Chemical Sciences, IISER-Kolkata, India.

<sup>e</sup> Supramolecular Chemistry Laboratory, New Chemistry Unit, Jawaharlal Nehru Centre for Advanced Scientific Research (JNCASR), Jakkur, Bangalore, India.

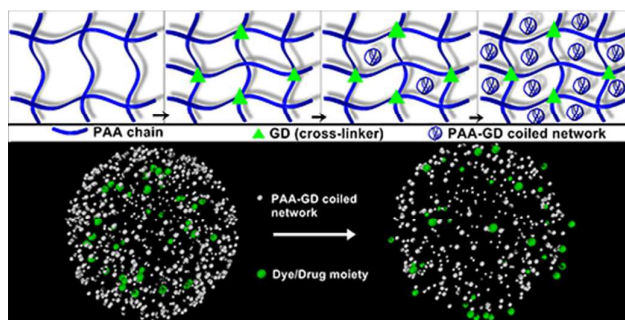
1. T. Xie, S. Li, Q. Peng and Y. Li, *Angew. Chem. Int. Ed.*, 2009, 48, 196-200.
2. I. Zhang, C. P. Royall, M. A. Faers and P. Bartlett, *Soft Matter*, 2013, 9, 2076-2084.
3. J. Sabin, A. E. Bailey, G. Espinosa and B. J. Frisken, *Phys. Rev. Lett.*, 2012, 109, 195701.
4. M. M. Baksh, M. Jaros and J. T. Groves, *Nature*, 2004, 427, 139-141.
5. F. Castro-Marcano, A. M. Cataño-Barrera and C. M. Colina, *Ind. Eng. Chem. Res.*, 2011, 50, 1046-1055.
6. G. Rodriguez, M. Cocera, L. Rubio, C. Alonso, R. Pons, C. Sandt, P. Dumas, C. Lopez-Iglesias, A. de la Maza and O. Lopez, *Phys. Chem. Chem. Phys.*, 2012, 14, 14523-14533.
7. H. N. W. Lekkerkerker, W. C. K. Poon, P. N. Pusey, A. Stroobants and P. B. Warren, *Europhys. Lett.*, 1992, 20, 559.
8. P. N. Pusey, W. Van Megen, S. M. Underwood, P. Bartlett and R. H. Ottewill, *Phys. A (Amsterdam, Neth.)*, 1991, 176, 16-27.
9. P. H. Poole, F. Sciortino, U. Essmann and H. E. Stanley, *Nature*, 1992, 360, 324-328.
10. D. J. Mitchell, G. J. T. Tiddy, L. Waring, T. Bostock and M. P. McDonald, *J. Chem. Soc., Faraday Trans. 1*, 1983, 79, 975-1000.
11. W. C. K. Poon, *Curr. Opin. Colloid Interface Sci.*, 1998, 3, 593-599.
12. V. J. Anderson and H. N. W. Lekkerkerker, *Nature*, 2002, 416, 811-815.
13. S. Roy, *Comments Inorg. Chem.*, 2011, 32, 113-126.
14. M. S. Romero-Cano and A. M. Puertas, *Soft Matter*, 2008, 4, 1242-1248.
15. K. J. Mutch, J. S. van Duijneveldt and J. Eastoe, *Soft Matter*, 2007, 3, 155-167.
16. L. Feng, B. Laderman, S. Sacanna and P. Chaikin, *Nat. Mater.*, 2015, 14, 61-65.
17. P.-G. de Gennes, *Nature*, 2001, 412, 385-385.
18. P. Jiang, J. F. Bertone and V. L. Colvin, *Science*, 2001, 291, 453-457.
19. B. Hartke, *Angew. Chem. Int. Ed.*, 2002, 41, 1468-1487.
20. N. L. McFarlane, N. J. Wagner, E. W. Kaler and M. L. Lynch, *Langmuir*, 2010, 26, 13823-13830.
21. R. Pandey and J. C. Conrad, *Soft Matter*, 2012, 8, 10695-10703.
22. D. J. Ashton and N. B. Wilding, *Phys. Rev. E*, 2014, 89, 031301.
23. G. D'Adamo, A. Pelissetto and C. Pierleoni, *J. Chem. Phys.*, 2014, 141, 244905.
24. K. J. Mutch, J. S. van Duijneveldt, J. Eastoe, I. Grillo and R. K. Heenan, *Langmuir*, 2010, 26, 1630-1634.
25. T. P. Russell, *Science*, 2013, 341, 1351-1352.
26. B. Tsang, C. Yu and S. Granick, *ACS Nano*, 2014, 8, 11030-11034.
27. C. V. Synatschke, T. I. Löbbling, M. Förtsch, A. Hanisch, F. H. Schacher and A. H. E. Müller, *Macromolecules*, 2013, 46, 6466-6474.
28. W.-F. Lai and H. C. Shum, *ACS Appl. Mater. Interfaces*, 2015, 7, 10501-10510.
29. S. V. Larin, A. A. Darinskii, E. B. Zhulina and O. V. Borisov, *Langmuir*, 2009, 25, 1915-1918.
30. T. V. Burova, N. V. Grinberg, D. R. Tur, V. S. Papkov, A. S. Dubovik, E. D. Shibanova, D. I. Bairamashvili, V. Y. Grinberg and A. R. Khokhlov, *Langmuir*, 2013, 29, 2273-2281.
31. D. V. Pergushov, A. H. E. Muller and F. H. Schacher, *Chem. Soc. Rev.*, 2012, 41, 6888-6901.
32. M. Tress, E. U. Mapesa, W. Kossack, W. K. Kipnusu, M. Reiche and F. Kremer, *Science*, 2013, 341, 1371-1374.
33. M. Terauchi, G. Ikeda, K. Nishida, A. Tamura, S. Yamaguchi, K. Harada and N. Yui, *Macromol. Biosci.*, 2015, 15, 953-964.
34. J. B. Matson, Y. Navon, R. Bitton and S. I. Stupp, *ACS Macro Lett.*, 2015, 4, 43-47.
35. Y. Anraku, A. Kishimura, Y. Yamasaki and K. Kataoka, *J. Am. Chem. Soc.*, 2013, 135, 1423-1429.
36. S. Gon and M. M. Santore, *Langmuir*, 2011, 27, 1487-1493.
37. Y. Zhao, R. Berger, K. Landfester and D. Crespy, *Polym. Chem.*, 2014, 5, 365-371.
38. I. Coluzza, P. D. J. van Oostrum, B. Capone, E. Reimhult and C. Dellago, *Phys. Rev. Lett.*, 2013, 110, 075501.
39. I. Coluzza, P. D. J. van Oostrum, B. Capone, E. Reimhult and C. Dellago, *Soft Matter*, 2013, 9, 938-944.
40. Y. Gi-Ra, J. P. David and S. Stefano, *J. Phys.: Condens. Matter*, 2013, 25, 193101.
41. S. Gon and M. M. Santore, *Langmuir*, 2011, 27, 15083-15091.
42. B. H. Tan and K. C. Tam, *Adv. Colloid Interface Sci.*, 2008, 136, 25-44.
43. A. J. Gormley, R. Chandrawati, A. J. Christofferson, C. Loynachan, C. Jumeaux, A. Artzy-Schnirman, D. Aili, I. Yarovsky and M. M. Stevens, *Chem. Mater.*, 2015, 27, 5820-5824.
44. S. Kiyonaka, S.-L. Zhou and I. Hamachi, *Supramol. Chem.*, 2003, 15, 521-528.
45. F. Ilmain, T. Tanaka and E. Kokufuta, *Nature*, 1991, 349, 400-401.
46. J. B. Rothbard, T. C. Jessop, R. S. Lewis, B. A. Murray and P. A. Wender, *J. Am. Chem. Soc.*, 2004, 126, 9506-9507.
47. M. D. Yilmaz and J. Huskens, *Soft Matter*, 2012, 8, 11768-11780.

48. Y. Wang, H. Xu and X. Zhang, *Adv. Mater.*, 2009, 21, 2849-2864.
49. L.-B. Meng, W. Zhang, D. Li, Y. Li, X.-Y. Hu, L. Wang and G. Li, *Chem. Commun.*, 2015, DOI: 10.1039/C5CC05785J.
50. K. R. Raghupathi, J. Guo, O. Munkhbat, P. Rangadurai and S. Thayumanavan, *Acc. Chem. Res.*, 2014, 47, 2200-2211.
51. F. Rodler, B. Schade, C. M. Jäger, S. Backes, F. Hampel, C. Böttcher, T. Clark and A. Hirsch, *J. Am. Chem. Soc.*, 2015, 137, 3308-3317.
52. B. J. Cafferty, R. R. Avirah, G. B. Schuster and N. V. Hud, *Chem. Sci.*, 2014, 5, 4681-4686.
53. C. Stoffelen and J. Huskens, *Nanoscale*, 2015, 7, 7915-7919.
54. W. Cao, Y. Gu, T. Li and H. Xu, *Chem. Commun.*, 2015, 51, 7069-7071.
55. X. Cai, L. Zhong, Y. Su, S. Lin and X. He, *Polym. Chem.*, 2015, 6, 3875-3884.
56. C. Maiti, R. Banerjee, S. Maiti and D. Dhara, *Langmuir*, 2015, 31, 32-41.
57. A. G. Baboul, L. A. Curtiss, P. C. Redfern and K. Raghavachari, *J. Chem. Phys.*, 1999, 110, 7650-7657.
58. K. V. Rao, K. Jayaramulu, T. K. Maji and S. J. George, *Angew. Chem. Int. Ed.*, 2010, 49, 4218-4222.
59. F. F. Xue, D. D. Yuan, A. Sahasrabudhe, S. Biswas, P. Wang, X.-Y. Tang, D. Chen, R. Yuan and S. Roy, *New J. Chem.*, 2012, 36, 2541-2548.
60. X. Su, S. Voskian, R. P. Hughes and I. Aprahamian, *Angew. Chem. Int. Ed.*, 2013, 52, 10734-10739.
61. R. E. Bulo, D. Donadio, A. Laio, F. Molnar, J. Rieger and M. Parrinello, *Macromolecules*, 2007, 40, 3437-3442.
62. L. de Campo, A. Yagmur, L. Sagalowicz, M. E. Leser, H. Watzke and O. Glatter, *Langmuir*, 2004, 20, 5254-5261.
63. J. Lyklema, *Fundamentals of Interface and Colloid Science: Solid-Liquid Interfaces*, Elsevier Science, 1995.
64. E. K. Hobbie, *Langmuir*, 1999, 15, 8807-8812.

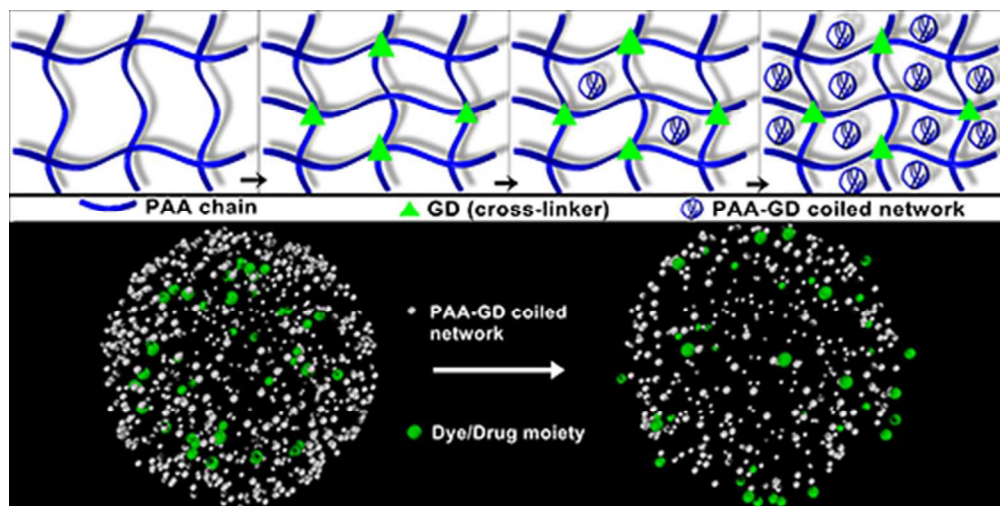
ARTICLE

Journal Name

## TOC Graphic



We synthesise a supramolecular polyelectrolyte complex consists of polyacrylic acid and guanidine which shows pH responsive phase transition and can carry functional moieties like drug and dye and release them in certain pH condition owing to pH dependent phase behaviour of the complex.



133x66mm (96 x 96 DPI)